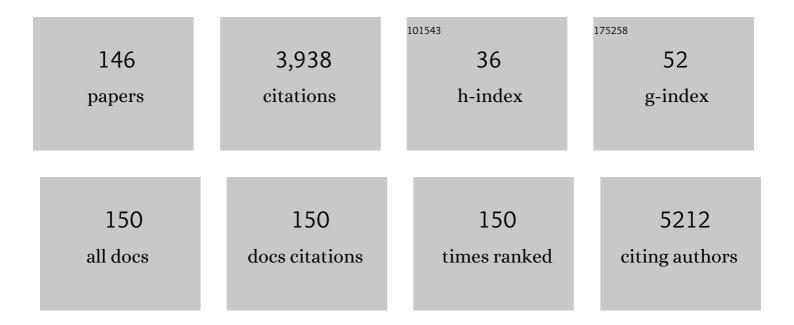
Huan Chen

List of Publications by Year in descending order

Source: https://exaly.com/author-pdf/1748092/publications.pdf Version: 2024-02-01



#	Article	IF	CITATIONS
1	A Prospective Study Comparing Cancer Detection Rates of Transperineal Prostate Biopsies Performed by Junior Urologists versus a Senior Consultant in a Real-World Setting. Urologia Internationalis, 2022, 106, 884-890.	1.3	1
2	Insights into the hydrated electron generation from UV/aniline: Mechanism and quantum efficiency. Chemosphere, 2022, 287, 132292.	8.2	4
3	Alterations in DNA damage response and repair genes as potential biomarkers for immune checkpoint blockade in gastrointestinal cancer. Cancer Biology and Medicine, 2022, 19, 1139-1149.	3.0	4
4	Time-dependent molecular progression and acute toxicity of oil-soluble, interfacially-active, and water-soluble species reveals their rapid formation in the photodegradation of Macondo Well Oil. Science of the Total Environment, 2022, 813, 151884.	8.0	7
5	PTI and ETI: convergent pathways with diverse elicitors. Trends in Plant Science, 2022, 27, 113-115.	8.8	72
6	Crop selection reduces potential heavy metal(loid)s health risk in wastewater contaminated agricultural soils. Science of the Total Environment, 2022, 819, 152502.	8.0	24
7	Chemical characterization of dissolved organic matter as disinfection byproduct precursors by UV/fluorescence and ESI FT-ICR MS after smoldering combustion of leaf needles and woody trunks of pine (Pinus jeffreyi). Water Research, 2022, 209, 117962.	11.3	9
8	Unveil the role of dissolved and sedimentary metal(loid)s on bacterial communities and metal resistance genes (MRGs) in an urban river of the Qinghai-Tibet Plateau. Water Research, 2022, 211, 118050.	11.3	22
9	Bi25FeO40/Bi2O2CO3 piezoelectric catalyst with built-in electric fields that was prepared via photochemical self-etching of Bi25FeO40 for 4-chlorophenol degradation. Journal of Cleaner Production, 2022, 341, 130908.	9.3	22
10	An open source computational workflow for the discovery of autocatalytic networks in abiotic reactions. Chemical Science, 2022, 13, 4838-4853.	7.4	8
11	Nitrogen Enrichment during Soil Organic Matter Burning and Molecular Evidence of Maillard Reactions. Environmental Science & Technology, 2022, 56, 4597-4609.	10.0	20
12	Impacts of haze on the photobleaching of chromophoric dissolved organic matter in surface water. Environmental Research, 2022, 212, 113305.	7.5	3
13	RNF7 inhibits apoptosis and sunitinib sensitivity and promotes glycolysis in renal cell carcinoma via the SOCS1/JAK/STAT3 feedback loop. Cellular and Molecular Biology Letters, 2022, 27, 36.	7.0	10
14	Linking the Jehol Biota Evolution to the Early Cretaceous Volcanism During the North China Craton Destruction: Insights From F, Cl, S, and P. Journal of Geophysical Research: Solid Earth, 2022, 127, .	3.4	3
15	Sustainable functional urethral reconstruction: Maximizing early continence recovery in robotic-assisted radical prostatectomy. Asian Journal of Urology, 2021, 8, 126-133.	1.2	6
16	Characterization of Dissolved Organic Matter from Wildfire-induced Microcystis aeruginosa Blooms controlled by Copper Sulfate as Disinfection Byproduct Precursors Using APPI(-) and ESI(-) FT-ICR MS. Water Research, 2021, 189, 116640.	11.3	23
17	Identification of immune checkpoint and cytokine signatures associated with the response to immune checkpoint blockade in gastrointestinal cancers. Cancer Immunology, Immunotherapy, 2021, 70, 2669-2679.	4.2	4
18	Molecular Comparison of Solid-Phase Extraction and Liquid/Liquid Extraction of Water-Soluble Petroleum Compounds Produced through Photodegradation and Biodegradation by FT-ICR Mass Spectrometry. Analytical Chemistry, 2021, 93, 4611-4618.	6.5	10

#	Article	IF	CITATIONS
19	Classification of the Biogenicity of Complex Organic Mixtures for the Detection of Extraterrestrial Life. Life, 2021, 11, 234.	2.4	12
20	A genomic mutation signature predicts the clinical outcomes of immunotherapy and characterizes immunophenotypes in gastrointestinal cancer. Npj Precision Oncology, 2021, 5, 36.	5.4	20
21	Transperineal Parallel Biopsy of the Prostate: A New Approach of Tissue Sampling for Precision Medicine. International Journal of General Medicine, 2021, Volume 14, 1631-1640.	1.8	1
22	CoO x @Coâ€NC Catalyst with Dual Active Centers for Enhanced Oxygen Evolution: Breaking Tradeâ€Off of Particle Size and Metal Loading. Chemistry - A European Journal, 2021, 27, 10657-10665.	3.3	6
23	Spatioâ€ŧemporal changes in dissolved organic matter composition along the salinity gradient of a marshâ€influenced estuarine complex. Limnology and Oceanography, 2021, 66, 3040-3054.	3.1	11
24	Case Report: A Squamous Cell Lung Carcinoma Patient Who Responded to Neoadjuvant Immunochemotherapy but Died From Anastomosis Leakage or/and irAEs: Immune Microenvironment and Genomic Features Changes. Frontiers in Oncology, 2021, 11, 674328.	2.8	1
25	Coupling sprinkler freshwater irrigation with vegetable species selection as a sustainable approach for agricultural production in farmlands with a history of 50-year wastewater irrigation. Journal of Hazardous Materials, 2021, 414, 125576.	12.4	8
26	TRIM27 interacts with lκbα to promote the growth of human renal cancer cells through regulating the NF-κB pathway. BMC Cancer, 2021, 21, 841.	2.6	12
27	Using watermelon rind and nitrite-containing wastewater for electricity production in a membraneless biocathode microbial fuel cell. Journal of Cleaner Production, 2021, 307, 127306.	9.3	12
28	Defect Regulating of Few-Layer Antimonene from Acid-Assisted Exfoliation for Enhanced Electrocatalytic Nitrogen Fixation. ACS Applied Materials & Interfaces, 2021, 13, 40618-40628.	8.0	14
29	Microplastics interaction with terrestrial plants and their impacts on agriculture. Journal of Environmental Quality, 2021, 50, 1024-1041.	2.0	43
30	Machine Learning for Identification of Primary Water Concentrations in Mantle Pyroxene. Geophysical Research Letters, 2021, 48, e2021GL095191.	4.0	5
31	Discovery of Oxygenated Hydrocarbon Biodegradation Products at a Late-Stage Petroleum Release Site. Energy & Fuels, 2021, 35, 16713-16723.	5.1	3
32	Germline HLA-B evolutionary divergence influences the efficacy of immune checkpoint blockade therapy in gastrointestinal cancer. Genome Medicine, 2021, 13, 175.	8.2	12
33	Two interacting transcriptional coactivators cooperatively control plant immune responses. Science Advances, 2021, 7, eabl7173.	10.3	31
34	Expanding the Analytical Window for Biochar Speciation: Molecular Comparison of Solvent Extraction and Water-Soluble Fractions of Biochar by FT-ICR Mass Spectrometry. Analytical Chemistry, 2021, 93, 15365-15372.	6.5	13
35	Parental choice of childcare in England: Choosing in phases and the split market. British Educational Research Journal, 2020, 46, 281-300.	2.5	3
36	Visible-light photocatalytic degradation of bisphenol A using cobalt-to-oxygen doped graphitic carbon nitride with nitrogen vacancies via metal-to-ligand charge transfer. Journal of Hazardous Materials, 2020, 384, 121247.	12.4	48

#	Article	IF	CITATIONS
37	Influence of the subduction of the Pacific plate on the mantle characteristics of South China: Constraints from the temporal geochemical evolution of the Mesozoic basalts in the Jitai Basin. Lithos, 2020, 352-353, 105253.	1.4	11
38	Experience of one single surgeon with the first 500 robot-assisted laparoscopic prostatectomy cases in mainland China. Asian Journal of Urology, 2020, 7, 170-176.	1.2	9
39	Re: Experience of one single surgeon with the first 500 robot-assisted laparoscopic prostatectomy cases in mainland China. Asian Journal of Urology, 2020, 7, 179-180.	1.2	0
40	Formation of assimilable organic carbon (AOC) during drinking water disinfection: A microbiological prospect of disinfection byproducts. Environment International, 2020, 135, 105389.	10.0	33
41	Hurricane resulted in releasing more nitrogenous than carbonaceous disinfection byproduct precursors in coastal watersheds. Science of the Total Environment, 2020, 705, 135785.	8.0	15
42	Molecular dynamics of foliar litter and dissolved organic matter during the decomposition process. Biogeochemistry, 2020, 150, 17-30.	3.5	8
43	Stereoselective and Divergent Construction of β-Thiolated/Selenolated Amino Acids via Photoredox-Catalyzed Asymmetric Giese Reaction. Journal of the American Chemical Society, 2020, 142, 14201-14209.	13.7	48
44	Prediction of immune checkpoint inhibition with immune oncology-related gene expression in gastrointestinal cancer using a machine learning classifier. , 2020, 8, e000631.		22
45	Characteristics of soil organic matter 14 years after a wildfire: A pyrolysis-gas-chromatography mass spectrometry (Py-GC-MS) study. Journal of Analytical and Applied Pyrolysis, 2020, 152, 104922.	5.5	8
46	Environmental Regulation of the Distribution and Ecology of Bdellovibrio and Like Organisms. Frontiers in Microbiology, 2020, 11, 545070.	3.5	21
47	Soil Organic Carbon Signature under Impervious Surfaces. ACS Earth and Space Chemistry, 2020, 4, 1785-1792.	2.7	12
48	Dynamics of dissolved organic matter and disinfection byproduct precursors along a low elevation gradient in woody wetlands - an implication of hydrologic impacts of climate change on source water quality. Water Research, 2020, 181, 115908.	11.3	19
49	Impact of Zero-Valent Iron Nanoparticles on <i>Fremyella diplosiphon</i> Transesterified Lipids and Fatty Acid Methyl Esters. ACS Omega, 2020, 5, 12166-12173.	3.5	9
50	Cyanobacteria as a biofuel source: advances and applications. , 2020, , 269-289.		8
51	A genomic and epigenomic atlas of prostate cancer in Asian populations. Nature, 2020, 580, 93-99.	27.8	183
52	Low water treatability efficiency of wildfire-induced dissolved organic matter and disinfection by-product precursors. Water Research, 2020, 184, 116111.	11.3	13
53	Molecular Transformation of Crude Oil Contaminated Soil after Bioelectrochemical Degradation Revealed by FT-ICR Mass Spectrometry. Environmental Science & Technology, 2020, 54, 2500-2509.	10.0	19
54	Metal-free 2D/2D heterojunction of covalent triazine-based frameworks/graphitic carbon nitride with enhanced interfacial charge separation for highly efficient photocatalytic elimination of antibiotic pollutants. Journal of Hazardous Materials, 2020, 391, 122204.	12.4	54

#	Article	IF	CITATIONS
55	Speciation and conversion of carbon and nitrogen in young landfill leachate during anaerobic biological pretreatment. Waste Management, 2020, 106, 88-98.	7.4	15
56	DNA Damage Repair Gene Mutations Are Indicative of a Favorable Prognosis in Colorectal Cancer Treated With Immune Checkpoint Inhibitors. Frontiers in Oncology, 2020, 10, 549777.	2.8	26
57	Hazardous substances as the dominant non-methane volatile organic compounds with potential emissions from liquid storage tanks during well fracturing: A modeling approach. Journal of Environmental Management, 2020, 268, 110715.	7.8	10
58	Short-term therapeutic outcomes of robotic-assisted laparoscopic radical prostatectomy for oligometastatic prostate cancer: a propensity score matching study. Chinese Medical Journal, 2020, 133, 127-133.	2.3	3
59	Enhanced photocatalytic disinfection of Escherichia coli K-12 by porous g-C3N4 nanosheets: Combined effect of photo-generated and intracellular ROSs. Chemosphere, 2019, 235, 1116-1124.	8.2	28
60	Shadow detection and removal in apple image segmentation under natural light conditions using an ultrametric contour map. Biosystems Engineering, 2019, 184, 142-154.	4.3	18
61	Clinical Benefit of Sorafenib Combined with Paclitaxel and Carboplatin to a Patient with Metastatic Chemotherapyâ€Refractory Testicular Tumors. Oncologist, 2019, 24, e1437-e1442.	3.7	4
62	Fabrication of two-dimensional indium oxide nanosheets with graphitic carbon nitride nanosheets as sacrificial templates. Materials Letters, 2019, 242, 24-27.	2.6	11
63	Throughfall Dissolved Organic Matter as a Terrestrial Disinfection Byproduct Precursor. ACS Earth and Space Chemistry, 2019, 3, 1603-1613.	2.7	19
64	Molecular-Level Characterization of Oil-Soluble Ketone/Aldehyde Photo-Oxidation Products by Fourier Transform Ion Cyclotron Resonance Mass Spectrometry Reveals Similarity Between Microcosm and Field Samples. Environmental Science & Technology, 2019, 53, 6887-6894.	10.0	43
65	Augmenting Fremyella diplosiphon Cellular Lipid Content and Unsaturated Fatty Acid Methyl Esters Via Sterol Desaturase Gene Overexpression. Applied Biochemistry and Biotechnology, 2019, 189, 1127-1140.	2.9	11
66	One-pot fabrication of a double Z-scheme CeCO ₃ OH/g-C ₃ N ₄ /CeO ₂ photocatalyst for nitrogen fixation under solar irradiation. Catalysis Science and Technology, 2019, 9, 2849-2857.	4.1	38
67	Three-Component Protein Modification Using Mercaptobenzaldehyde Derivatives. Organic Letters, 2019, 21, 3828-3833.	4.6	12
68	Atmospheric Pressure Photoionization Fourier Transform Ion Cyclotron Resonance Mass Spectrometry Characterization of Oil Sand Process-Affected Water in Constructed Wetland Treatment. Energy & Fuels, 2019, 33, 4420-4431.	5.1	8
69	Control wildfire-induced Microcystis aeruginosa blooms by copper sulfate: Trade-offs between reducing algal organic matter and promoting disinfection byproduct formation. Water Research, 2019, 158, 227-236.	11.3	52
70	Graphitic carbon nitride grown in situ on aldehyde-functionalized α-Fe2O3: All-solid-state Z-scheme heterojunction for remarkable improvement of photo-oxidation activity. Journal of Colloid and Interface Science, 2019, 548, 284-292.	9.4	29
71	Nuclear Receptor Coactivator 2 Promotes Human Breast Cancer Cell Growth by Positively Regulating the MAPK/ERK Pathway. Frontiers in Oncology, 2019, 9, 164.	2.8	18
72	Palladium-Catalyzed Stereospecific <i>C</i> -Glycosylation of Glycals with Vinylogous Acceptors. ACS Catalysis, 2019, 9, 2909-2915.	11.2	36

#	Article	IF	CITATIONS
73	Oxidative phenol-arene and phenol-phenol cross-coupling using periodic acid. Tetrahedron, 2019, 75, 2004-2011.	1.9	5
74	Direct electricity production from subaqueous wetland sediments and banana peels using membrane-less microbial fuel cells. Industrial Crops and Products, 2019, 128, 70-79.	5.2	16
75	Visible light photocatalytic mineralization of bisphenol A by carbon and oxygen dual-doped graphitic carbon nitride. Journal of Colloid and Interface Science, 2019, 540, 97-106.	9.4	32
76	General Equilibrium Analysis of the Cobenefits and Trade-Offs of Carbon Mitigation on Local Industrial Water Use and Pollutants Discharge in China. Environmental Science & Technology, 2019, 53, 1715-1724.	10.0	28
77	All-solid-state Z-scheme Co9S8/graphitic carbon nitride photocatalysts for simultaneous reduction of Cr(VI) and oxidation of 2,4-dichlorophenoxyacetic acid under simulated solar irradiation. Chemical Engineering Journal, 2019, 360, 1188-1198.	12.7	63
78	Long-term watershed management is an effective strategy to reduce organic matter export and disinfection by-product precursors in source water. International Journal of Wildland Fire, 2019, 28, 804.	2.4	4
79	Corrigendum to: Long-term watershed management is an effective strategy to reduce organic matter export and disinfection by-product precursors in source water. International Journal of Wildland Fire, 2019, 28, 822.	2.4	2
80	Detailed Compositional Characterization of the 2014 Bangladesh Furnace Oil Released into the World's Largest Mangrove Forest. Energy & Fuels, 2018, 32, 3232-3242.	5.1	17
81	Coupling of sterically demanding peptides by β-thiolactone-mediated native chemical ligation. Chemical Science, 2018, 9, 1982-1988.	7.4	18
82	Comprehensive Analysis of Changes in Crude Oil Chemical Composition during Biosouring and Treatments. Environmental Science & Technology, 2018, 52, 1290-1300.	10.0	15
83	Traceless β-mercaptan-assisted activation of valinyl benzimidazolinones in peptide ligations. Chemical Science, 2018, 9, 1940-1946.	7.4	19
84	Multi-scale Spatial Patterns and Influencing Factors of Rural Poverty: A Case Study in the Liupan Mountain Region, Gansu Province, China. Chinese Geographical Science, 2018, 28, 296-312.	3.0	21
85	Dynamics of multiple elements in fast decomposing vegetable residues. Science of the Total Environment, 2018, 616-617, 614-621.	8.0	20
86	Origin, Reactivity, and Bioavailability of Mercury in Wildfire Ash. Environmental Science & Technology, 2018, 52, 14149-14157.	10.0	25
87	Construction of Acetaldehyde-Modified g-C ₃ N ₄ Ultrathin Nanosheets via Ethylene Glycol-Assisted Liquid Exfoliation for Selective Fluorescence Sensing of Ag ⁺ . ACS Applied Materials & Interfaces, 2018, 10, 44624-44633.	8.0	37
88	Wildfire Burn Intensity Affects the Quantity and Speciation of Polycyclic Aromatic Hydrocarbons in Soils. ACS Earth and Space Chemistry, 2018, 2, 1262-1270.	2.7	39
89	Liquid-phase hydrogenation of N-nitrosodimethylamine over Pd-Ni supported on CeO2-TiO2: The role of oxygen vacancies. Colloids and Surfaces A: Physicochemical and Engineering Aspects, 2018, 558, 211-218.	4.7	9
90	Electricity generation from different wetlands: Mechanisms based on dissolved organic matters in membrane-less microbial fuel cells. Chemical Engineering Journal, 2018, 351, 1006-1012.	12.7	10

#	Article	IF	CITATIONS
91	Modeling the carbon-energy-water nexus in a rapidly urbanizing catchment: A general equilibrium assessment. Journal of Environmental Management, 2018, 225, 93-103.	7.8	32
92	Children's Evaluation of the Physical Environment Quality in Kindergarten: A Case Study from China. International Journal of Early Childhood, 2018, 50, 175-192.	1.0	4
93	Integration of an automated identification-quantification pipeline and statistical techniques for pyrolysis GC/MS tracking of the molecular fingerprints of natural organic matter. Journal of Analytical and Applied Pyrolysis, 2018, 134, 371-380.	5.5	11
94	Bismuth Subcarbonate with Designer Defects for Broad-Spectrum Photocatalytic Nitrogen Fixation. ACS Applied Materials & Interfaces, 2018, 10, 25321-25328.	8.0	97
95	Composition-Dependent Sorptive Fractionation of Anthropogenic Dissolved Organic Matter by Fe(III)-Montmorillonite. Soil Systems, 2018, 2, 14.	2.6	25
96	Fremyella diplosiphon as a Biodiesel Agent: Identification of Fatty Acid Methyl Esters via Microwave-Assisted Direct In Situ Transesterification. Bioenergy Research, 2018, 11, 528-537.	3.9	13
97	Fractionation and mobility risks of heavy metals and metalloids in wastewater-irrigated agricultural soils from greenhouses and fields in Gansu, China. Geoderma, 2018, 328, 1-9.	5.1	64
98	Relative Contributions of Halobacteriovorax and Bacteriophage to Bacterial Cell Death under Various Environmental Conditions. MBio, 2018, 9, .	4.1	17
99	Modeling potential occupational inhalation exposures and associated risks of toxic organics from chemical storage tanks used in hydraulic fracturing using AERMOD. Environmental Pollution, 2017, 224, 300-309.	7.5	28
100	Fourier Transform Ion Cyclotron Resonance Mass Spectrometry Characterization of Athabasca Oil Sand Process-Affected Waters Incubated in the Presence of Wetland Plants. Energy & Fuels, 2017, 31, 1731-1740.	5.1	25
101	Heterogeneous source components of intraplate basalts from NE China induced by the ongoing Pacific slab subduction. Earth and Planetary Science Letters, 2017, 459, 208-220.	4.4	67
102	Characterization of the chemicals used in hydraulic fracturing fluids for wells located in the Marcellus Shale Play. Journal of Environmental Management, 2017, 200, 312-324.	7.8	36
103	Spatial variation of multiple air pollutants and their potential contributions to all-cause, respiratory, and cardiovascular mortality across China in 2015–2016. Atmospheric Environment, 2017, 168, 23-35.	4.1	46
104	Typical oxygen isotope profile of altered oceanic crust recorded in continental intraplate basalts. Journal of Earth Science (Wuhan, China), 2017, 28, 578-587.	3.2	5
105	Adsorptive fractionation of dissolved organic matter (DOM) by mineral soil: Macroscale approach and molecular insight. Organic Geochemistry, 2017, 103, 113-124.	1.8	102
106	The noncoding RNA HOXD-AS1 is a critical regulator of the metastasis and apoptosis phenotype in human hepatocellular carcinoma. Molecular Cancer, 2017, 16, 125.	19.2	76
107	Robotic-assisted Laparoscopic Radical Prostatectomy From a Single Chinese Center: A Learning Curve Analysis. Urology, 2016, 93, 104-111.	1.0	16
108	4 Years after the <i>Deepwater Horizon</i> Spill: Molecular Transformation of Macondo Well Oil in Louisiana Salt Marsh Sediments Revealed by FT-ICR Mass Spectrometry. Environmental Science & Technology, 2016, 50, 9061-9069.	10.0	66

#	Article	IF	CITATIONS
109	Total synthesis of atropurpuran. Nature Communications, 2016, 7, 12183.	12.8	52
110	Applications of comprehensive two-dimensional gas chromatography (GCÂ×ÂGC) inÂstudying the source, transport, andÂfate of petroleum hydrocarbons inÂthe environment. , 2016, , 399-448.		20
111	Photochemical changes in water accommodated fractions of MC252 and surrogate oil created during solar exposure as determined by FT-ICR MS. Marine Pollution Bulletin, 2016, 104, 262-268.	5.0	34
112	Water usage for natural gas production through hydraulic fracturing in the United States from 2008 to 2014. Journal of Environmental Management, 2016, 170, 152-159.	7.8	78
113	Synthetic approach to the functionalized tricyclic core of atropurpuran. Tetrahedron, 2016, 72, 347-353.	1.9	11
114	<i>Halobacteriovorax,</i> an underestimated predator on bacteria: potential impact relative to viruses on bacterial mortality. ISME Journal, 2016, 10, 491-499.	9.8	58
115	Recycled oceanic crust and marine sediment in the source of alkali basalts in Shandong, eastern China: Evidence from magma water content and oxygen isotopes. Journal of Geophysical Research: Solid Earth, 2015, 120, 8281-8303.	3.4	41
116	Draft genome sequences for the obligate bacterial predators Bacteriovorax spp. of four phylogenetic clusters. Standards in Genomic Sciences, 2015, 10, 11.	1.5	12
117	Total Syntheses of (â^')â€Isoschizogamine and (â^')â€2â€Hydroxyisoschizogamine. Chemistry - A European Journal, 2015, 21, 14602-14607.	3.3	22
118	An Integrated Approach for the Identification of HNF4α-Centered Transcriptional Regulatory Networks During Early Liver Regeneration. Cellular Physiology and Biochemistry, 2015, 36, 2317-2326.	1.6	10
119	Downregulation of IL6 Targeted MiR-376b May Contribute to a Positive IL6 Feedback Loop During Early Liver Regeneration in Mice. Cellular Physiology and Biochemistry, 2015, 37, 233-242.	1.6	16
120	Changing recycled oceanic components in the mantle source of the Shuangliao Cenozoic basalts, NE China: New constraints from water content. Tectonophysics, 2015, 650, 113-123.	2.2	56
121	Unprecedented Insights into the Chemical Complexity of Coal Tar from Comprehensive Two-Dimensional Gas Chromatography Mass Spectrometry and Direct Infusion Fourier Transform Ion Cyclotron Resonance Mass Spectrometry. Energy & Fuels, 2015, 29, 641-648.	5.1	33
122	Genome-wide comparative analysis of ABC systems in the Bdellovibrio-and-like organisms. Gene, 2015, 562, 132-137.	2.2	5
123	Water Content and Oxygen Isotopic Composition of Alkali Basalts from the Taihang Mountains, China: Recycled Oceanic Components in the Mantle Source. Journal of Petrology, 2015, 56, 681-702.	2.8	60
124	MiR-376a and Histone Deacetylation 9 Form A Regulatory Circuitry in Hepatocellular Carcinoma. Cellular Physiology and Biochemistry, 2015, 35, 729-739.	1.6	32
125	Water content of the Xiaogulihe ultrapotassic volcanic rocks, NE China: implications for the source of the potassium-rich component. Science Bulletin, 2015, 60, 1468-1470.	9.0	14
126	Temporal variation of H 2 O content in the lithospheric mantle beneath the eastern North China Craton: Implications for the destruction of cratons. Gondwana Research, 2015, 28, 276-287.	6.0	32

Huan Chen

#	Article	IF	CITATIONS
127	MicroRNA-127 Post-Transcriptionally Downregulates Sept7 and Suppresses Cell Growth in Hepatocellular Carcinoma Cells. Cellular Physiology and Biochemistry, 2014, 33, 1537-1546.	1.6	54
128	Partial melting control of water contents in the Cenozoic lithospheric mantle of the Cathaysia block of South China. Chemical Geology, 2014, 380, 7-19.	3.3	49
129	An integrated approach for the identification of USF1-centered transcriptional regulatory networks during liver regeneration. Biochimica Et Biophysica Acta - Gene Regulatory Mechanisms, 2014, 1839, 415-423.	1.9	6
130	Sunlight creates oxygenated species in water-soluble fractions of Deepwater horizon oil. Journal of Hazardous Materials, 2014, 280, 636-643.	12.4	83
131	Inhibition of glycogen synthase kinase 3 ameliorates liver ischemia/reperfusion injury via an energy-dependent mitochondrial mechanism. Journal of Hepatology, 2014, 61, 816-824.	3.7	31
132	Niche Partition of Bacteriovorax Operational Taxonomic Units Along Salinity and Temporal Gradients in the Chesapeake Bay Reveals Distinct Estuarine Strains. Microbial Ecology, 2013, 65, 652-660.	2.8	18
133	A small predatory core genome in the divergent marine <i>Bacteriovorax marinus</i> SJ and the terrestrial <i>Bdellovibrio bacteriovorus</i> . ISME Journal, 2013, 7, 148-160.	9.8	43
134	Design and Synthesis of Cyclopropylamide Analogues of Combretastatin-A4 as Novel Microtubule-Stabilizing Agents. Journal of Medicinal Chemistry, 2013, 56, 685-699.	6.4	58
135	Synthesis of the atropurpuran A-ring via an organocatalytic asymmetric intramolecular Michael addition. Tetrahedron, 2013, 69, 3141-3148.	1.9	18
136	SD118-Xanthocillin X (1), a Novel Marine Agent Extracted from Penicillium commune, Induces Autophagy through the Inhibition of the MEK/ERK Pathway. Marine Drugs, 2012, 10, 1345-1359.	4.6	39
137	miRâ€376a suppresses proliferation and induces apoptosis in hepatocellular carcinoma. FEBS Letters, 2012, 586, 2396-2403.	2.8	70
138	Predatory Bacteriovorax Communities Ordered by Various Prey Species. PLoS ONE, 2012, 7, e34174.	2.5	40
139	Sharing of Prey: Coinfection of a Bacterium by a Virus and a Prokaryotic Predator. MBio, 2012, 3, e00051-12.	4.1	29
140	Down-Regulation of MiR-127 Facilitates Hepatocyte Proliferation during Rat Liver Regeneration. PLoS ONE, 2012, 7, e39151.	2.5	60
141	Prey bacteria shape the community structure of their predators. ISME Journal, 2011, 5, 1314-1322.	9.8	98
142	Mir-34a Is Upregulated during Liver Regeneration in Rats and Is Associated with the Suppression of Hepatocyte Proliferation. PLoS ONE, 2011, 6, e20238.	2.5	73
143	Impact of extracellular polymeric substances on the settlement ability of aerobic granular sludge. Environmental Technology (United Kingdom), 2010, 31, 1601-1612.	2.2	57
144	Nuclear factor κB participates in liver regeneration through regulating immediate early response 2. Academic Journal of Second Military Medical University, 2010, 30, 123-127.	0.0	0

#	Article	IF	CITATIONS
145	Inhibition of GSK-3β decreases NF-κB-dependent gene expression and impairs the rat liver regeneration. Journal of Cellular Biochemistry, 2007, 102, 1281-1289.	2.6	29
146	Structural Dependence of Photogenerated Transformation Products for Aromatic Hydrocarbons Isolated from Petroleum. Energy & Fuels, 0, , .	5.1	2